

## The role of core/shell-microparticle dispersions in polypropylene/polyamide-6 blends

Joachim Rösch\* and Rolf Mülhaupt

Freiburger Materialforschungszentrum und Institut für Makromolekulare Chemie der Albert-Ludwigs-Universität, Stefan-Meier-Strasse 21, D-79104 Freiburg, Germany

### Summary

Reactive blending of 70 vol.-% polypropylene (PP) and 30 vol.-% polyamide-6 (PA-6) was performed in the presence of various amounts of succinic-anhydride-functional elastomers which are immiscible with both blend components. Characteristic morphological feature of the resulting multiphase polymer blends was a continuous polypropylene matrix containing dispersed core/shell microparticles with rigid polyamide-6 core and soft elastomer shell. Accumulation of the elastomer component at the polypropylene/polyamide-6 interface and reaction of the succinic anhydride of the elastomer with the amine-endgroups of PA-6 enhanced PA-6 dispersion and proved to be the key to unusual property synergisms. In contrast to the conventional soft maleic-anhydride-grafted EPM elastomer (EPM-g-MAH), the stiffer maleic-anhydride-grafted poly[styrene-*b*-(ethene-co-butene-1)-*b*-styrene] (SEBS-g-MAH) was much more efficient as blend compatibilizer and gave PP/PA-6 blends with greatly improved strength and toughness without sacrificing stiffness.

### Introduction

The controlled formation of core/shell-microparticle dispersions plays an important role in the development of multiphase polymer blends exhibiting improved toughness. In principle two synthetic approaches have been introduced to achieve controlled formation of core/shell microparticle dispersions in a polymeric matrix. Firstly, in particle-forming polymerization processes elastomer microparticles are formed and grafted with thermoplastics to improve interfacial adhesion between the rubber microparticles and the thermoplastic matrix. Well-known examples are conventional rubber-toughened thermoplastics such as high impact polystyrene (1,2) and ABS (3). This approach has led to a variety of generations of impact modifiers prepared in emulsion polymerization processes (4). Secondly, new concepts based upon reactive processing are being developed to generate well-defined core/shell-type microparticles during melt-processing of thermoplastic polymer blends. For example, ternary blends of PMMA with PBT and PC (5) phase separate during processing to form dispersed PMMA microparticles encapsulated in a PC shell. Another important example are rigid filler microparticles which are coated with elastomers to enhance interfacial adhesion, thus improving toughness and stiffness (6).

The main advantage of incorporating rigid cores or subinclusions into elastomer microparticles is to reduce the effective elastomer volume fraction required to achieve a certain impact strength. As an illustration, the polystyrene subinclusions in HIPS increase the total elastomer volume fraction by a factor of 3-4 (7). With core/shell microparticles as local stress concentrators it is possible to improve toughness of thermoplastic and

\*Corresponding author

thermosetting materials (8). Rubber microparticles covalently attached to the polymeric matrix efficiently transfer stresses and dissipate energy at the crack tips. Moreover, similar to the role of carbon-black fillers in conventional rubbers, rigid cores and subinclusions represent reinforcing agents for elastomer microparticles. In contrast to the dispersion of soft rubber microparticles, the dispersions of the more rigid reinforced microparticles are known to give higher toughness without sacrificing stiffness.

Microparticle intercalations with the polymer matrix and their influence on mechanical blend properties are governed by the thickness of the elastomeric shell with respect to that of the rigid core, total microparticle volume fraction, mechanical properties and polymer compatibilities of core, shell and polymer matrix. Objective of our research is to develop reactive blending technologies for ternary blends comprising polar and hydrocarbon thermoplastic components which are combined with a non-polar elastomer acting as blend compatibilizer. Provided that all three components are mutually immiscible, the elastomeric component accumulates at the interfaces between the polar and non-polar components which are added in excess with respect to the elastomer. In order to improve the interfacial adhesion of the non-polar elastomer with the polar blend component, succinic-anhydride groups are attached to the elastomer backbone via maleic-anhydride grafting. Such anhydride groups react with endgroups of the polar polymer to covalently bond elastomer shell onto the polar core.

For the fundamental examination of core/shell-modified thermoplastics polypropylene (PP) was selected as the hydrocarbon blend component and polyamide-6 (PA-6) as the polar thermoplastic component. As elastomeric compatibilizers maleic-anhydride-grafted elastomers such as ethene/propene (EPM-g-MAH) and poly[styrene-*b*-(ethene-co-butene-1)-*b*-styrene] (SEBS-g-MAH) were applied. During melt-processing the anhydride groups react with the amine endgroups of the PA-6 to form imide-coupled block copolymers which improve compatibility of the elastomeric shell and the PA-6 core. Morphological and mechanical properties of the PP/PA-6 (70/30) blends were examined as a function of the elastomer types and volume fractions.

## Experimental

All polymers were commercial products and used without further purification. PP (Hostalen PPN 1060,  $M_n = 63.000$  g/mol,  $M_w = 182700$  g/mol determined by GPC in 1,2,4 trichlorobenzene at 135°C, PS-standards, MFI (230/2.16) = 2 dg/min,  $T_m = 165$  °C) was purchased from Hoechst AG. PA-6 (Sniamid ASN 27,  $M_n = 32000$  g/mol,  $T_m = 222$ °C) was supplied by Snia. Maleic-anhydride-grafted EPM (Exxelor VA 1803, 60 mmol MAH/kg, MFI (230/2.16) = 3 dg/min,  $T_g = -52$  °C) was a product of Exxon Chemicals. Maleic-anhydride grafted SEBS (Kraton G 1901 X2, 208 mmol MAH/kg, MFI (230/2.16) = 3,2 dg/min) was supplied by Shell Chemicals Co.

The PP/PA-6 blend consisted of 70 vol.-% of polypropylene and 30 vol.-% of a dispersed PA-6 phase. As the volume-fraction of the elastomeric compatibilizers increased, the PP volume fraction was reduced accordingly to maintain 30 vol.-% PA-6 and a total of (PP + elastomer) of 70 vol.-% (cf. Table 1).

All blends were prepared under identical mixing and molding conditions. PA-6 was dried for 6 hours at 80°C under oil pump vacuum prior to use. Melt blending was performed in a Haake Rheomix 90 equipped with a 60 ml mixing chamber, preheated at 240 °C. 40 g of the polymer blend, including 0,2 g stabilizer (80 % Irganox 1010 / 20 % Irgafos 168 (both from Ciba Geigy AG)), were kneaded for 4 min at 60 rpm. Temperature was checked by a thermocouple placed in the melt. The blend was removed quickly and quenched to room temperature. Sheets of 1,5 mm thickness were prepared by compression moulding in an evacuated press (Schwabenthan Polystat 100) after annealing at 260°C for 10 min and quenching to room temperature between water cooled metal plates.

For tensile testing dumbbell-shaped tensile bars according to DIN 53455 were cut and machined. Stress/strain tests to determine Young's modulus and yield stress were performed at 10 mm/min crosshead speed on an Instron 4204 at 23 °C. Notched Charpy impact strength was determined according to DIN 53453 on a Zwick 5102 equipped with 2 J pendulum using 5 test specimen. Morphological studies were carried out using the Zeiss CEM 902 transmission electron microscope. Thin sections, suitable for transmission electron microscope, were obtained after staining and hardening the samples in ruthenium tetroxide vapors for 6 hours. Microtoming of the samples into sections of 80 to 100 nm thickness was performed using an Reichert Jung Ultracut E equipped with a diamond knife.

## Results and Discussion

Polypropylene (PP) was melt-blended together with polyamide-6 (PA-6) at 70/30 volume fraction ratio in a blender at 240 °C. Maleic-anhydride-grafted elastomers such as ethene/propene (EPM-g-MAH) and poly[styrene-*b*-(ethene-co-butene)-*b*-styrene] (SEBS-g-MAH) were added as compatibilizers with concentrations varying between 0 and 20 vol.-%. As the elastomeric volume fraction increased, the volume fraction of PP was reduced accordingly to maintain a total of 30 vol.-% PA-6. The results are summarized in Table 1. Figure 1 shows the average diameter of the PA-6 microparticles dispersed in the PP matrix as a function of the elastomeric compatibilizer volume fraction. This clearly demonstrates that both compatibilizers are efficient dispersing agents. In the absence of the elastomeric component, the PP/PA-6 blend contained large irregularly shaped PA-6 microparticles and failed when exposed to small mechanical stresses. With increasing volume fraction of elastomer components the average PA-6 microparticle diameter was reduced by one order of magnitude. While 2.5 vol.-% SEBS-g-MAH was sufficient to reduce the PA-6 domain size to 0.6 µm, more than 10 vol.-% EPM-g-MAH was required to reach the same PA-6 domain-size level.

Table 1. PA-6 domain size and mechanical properties in 70 vol.-% PP/30 vol.-% PA-6 blends as a function of maleic-anhydride-grafted elastomer content

Elastomer Type	Elastomer Content (vol.-%)	PA-6 Domain Size (µm)	Young's Modulus (MPa)	Yield-Stress (MPa)	Notched Charpy Impact Strength (kJ/m <sup>2</sup> )
none	0	30	1350	22	3
EPM-g-MAH	2.5	15	1140	22	7
	5	4	1000	20	12
	10	0.7	730	16	31
	15	0.5	570	14	55
	20	0.3	370	13	100
SEBS-g-MAH	6	0.6	1250	35	18
	5	0.3	1060	32	25
	10	0.25	1000	30	40
	15	0.2	910	27	90
	20	0.15	780	24	no failure

A typical blend morphology, imaged by transmission electron microscopy, is shown in Figure 2 for PP/PA-6 (70/30) compatibilized with 5 vol.-% maleic-anhydride-grafted elastomer. Both elastomeric compatibilizers produce core/shell-microparticle dispersions of PA-6 microparticles encapsulated in an elastomeric shell. In the TEM micrographs, the elastomeric shells are preferentially stained with  $\text{RuO}_4$  and therefore appear darker in comparison to the PP matrix and the PA-6 core. This clearly indicates that both elastomeric compatibilizers are accumulated at the PP/PA-6 interfaces. No separate elastomeric microphases were found in the PP matrix. At 5 vol.-% EPM-g-MAH content a bimodal distribution of microparticles with PA-6 average domain sizes of approximately 4  $\mu\text{m}$  and 0.2  $\mu\text{m}$  were detected. In contrast, the same amount of the SEBS-g-MAH compatibilizers generated very uniform core/shell microparticles with PA-6 domains of 0.3  $\mu\text{m}$  average diameter. Interestingly, although the PA-6 remains separated by the SEBS shells, the PA-6/SEBS core/shell-microparticles formed agglomerates similar to honeycomb-like structures. At 20 vol.-% SEBS-g-MAH content, which is equivalent to 50 vol.-% PA-6/SEBS core/shell-microparticles, cocontinuous structures with PP and PA-6/SEBS were generated whereas the EPM-g-MAH compatibilizer did not produce such cocontinuous multiphase polymers over the entire EPM-g-MAH concentration range.

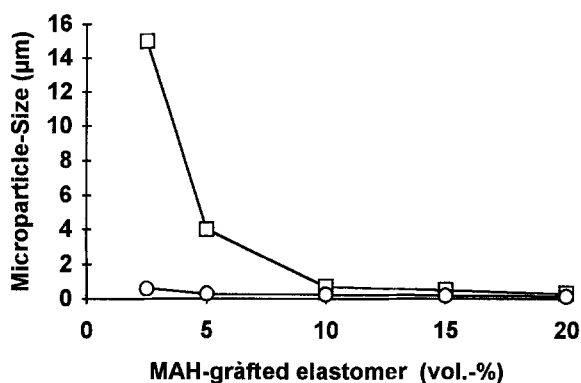


Figure 1. PA-6 domain diameter of PP/PA-6 (70/30) blends for various volume fractions of EPM-g-MAH ( $\square$ ) and SEBS-g-MAH ( $\circ$ ).

The variation of the mixing parameters such as temperature, hold-up time, screw revolving speed, indicate that the blend formation, i.e., the development of the typical blend morphologies as shown in Figure 2, was completed within a few minutes. The temperature range, however, is restricted to temperatures around 240  $^{\circ}\text{C}$ , because at higher temperatures thermo-oxidative degradation of PP as well as PA-6 affected the blend properties. This result is consistent with studies by Scott and Macosko (9) on Nylon/polystyrene blends where the dispersion process is completed after blending for the duration of two to three minutes.

The efficiency of the compatibilizers as dispersing agents, responsible for the dispersion of PA-6 in polypropylene melts, is related to the formation of elastomer/PA-6 graft copolymers during melt-blending. Such graft copolymers are produced when the amine-endgroups of PA-6 react with the pendant succinic-anhydride groups of the maleic-anhydride-grafted elastomers. When the amphiphilic graft copolymers accumulate at the PP/PA-6 interfaces, interfacial tensions decrease, thus causing better dispersion of the PA-6 in PP melts.

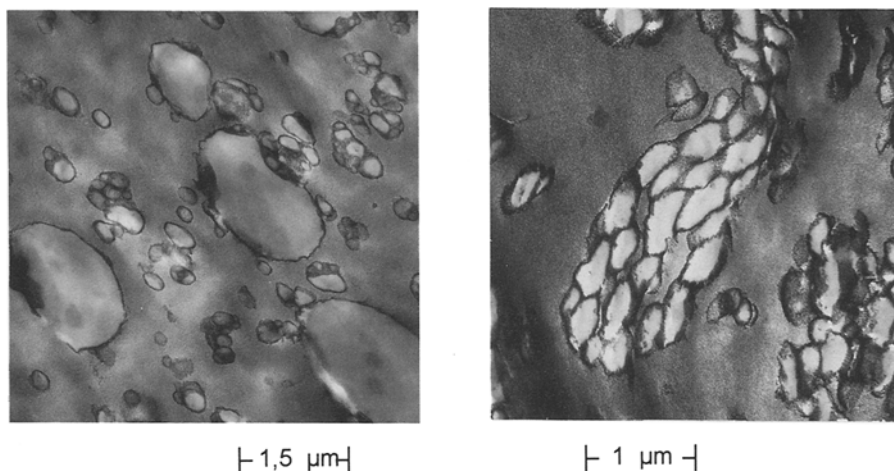


Figure 2. TEM images of  $\text{RuO}_4$ -stained PP/PA-6 (70/30) blends containing 5 vol.-% EPM-g-MAH (left) and 5 vol.-% SEBS-g-MAH (right).

The higher dispersing agent efficiency of SEBS-g-MAH versus EPM-g-MAH may result from the polymer compatibility differences between PP and the maleic-anhydride-grafted elastomers. While EPM-g-MAH is more compatible with PP, the less compatible SEBS-g-MAH appears to possess the optimal compatibility difference to accumulate at the interfaces and provide excellent adhesion to both PP and PA-6.

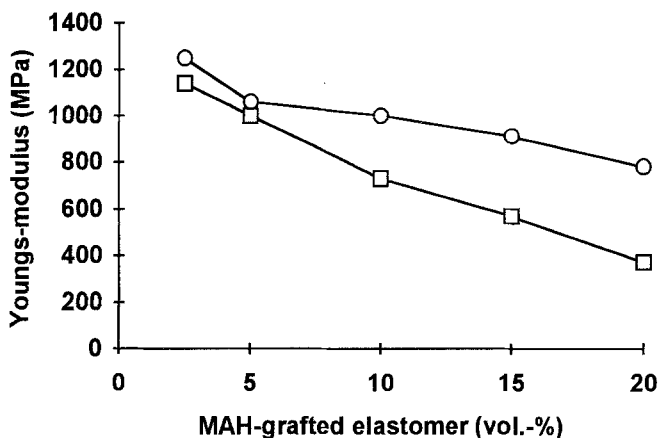


Figure 3. Influence of SEBS-g-MAH- (□) and EPM-g-MAH- (○) addition on the Young's modulus of PP/PA-6 (70/30) blends.

In addition to the PA-6 dispersion in PP-melts, the elastomeric blend compatibilizers also influence the solid-state properties of the PP/PA-6 blends. The Young's modulus, yield stress and notched Charpy impact strength of PP/PA-6 (70/30) were examined as a function of the types and volume fractions of the elastomeric compatibilizers. Since both compatibilizers are elastomers, the addition of such elastomeric blend components is expected to adversely affect the stiffness of the PP/PA-6 blends. In fact, as shown in Figure 3, the addition of 10 vol.-% EPM-g-MAH reduced the Young's modulus to 730 MPa. Interestingly, the same amount of SEBS-g-MAH gave a markedly higher Young's modulus of 1000 MPa which comparable to that of the non-modified PP matrix. Moreover, the Young's modulus decay was much stronger in the case of EPM-g-MAH-addition. Since in both cases the blend morphology types are comparable, this unusual behavior may result from the different Young's moduli of the elastomeric shells. The higher Young's modulus of SEBS of 100 MPa in comparison to 4 MPa of EPM yields stiffer elastomer shells which also account for the higher total stiffness of the blend.

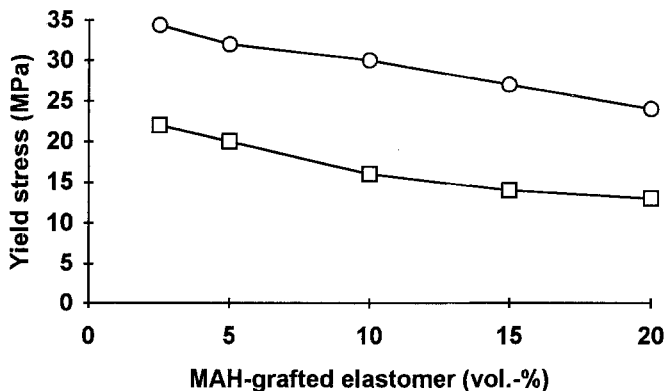


Figure 4. Influence of SEBS-g-MAH- (□) and EPM-g-MAH- (○) addition on the yield stress of PP/PA-6 (70/30) blends.

While the Young's modulus reflects the stiffness of the PP/PA-6 polymer blends, the yield stresses are related to the interfacial adhesion. In the absence of interfacial adhesion, Nielsen has demonstrated that yield stress decreases with a 2/3 power of the volume fraction of the dispersed phase(10). From Figure 4 it is apparent that EPM-g-MAH-modified PP/PA-6 blends give much smaller yield stresses when compared to the corresponding SEBS-g-MAH-based blends. With respect to the PP matrix with a yield stress of 32 MPa, the incorporation of the microparticles with PA-6 core and soft EPM shell gave drastically lower yield stresses. In sharp contrast, the SEBS-based PP/PA-6 blends displayed substantially higher yield stresses in the range of 25 to 35 MPa. In the case of SEBS-g-MAH-compatible PP/PA-6 blends, the efficient transfer of mechanical stresses between PP matrix and dispersed PA-6 microparticles appears to be much more efficient as a result of better interfacial adhesion in comparison to EPM-g-MAH-based PP/PA-6 blends.

This stress transfer also depends upon the nature of the elastomer shell. When compared to EPM-g-MAH the SEBS-g-MAH provides much higher strength because the resulting SEBS shell is physically crosslinked via the phase segregation of the SEBS

triblock copolymer. In EPM shells, there exist only transient crosslinks resulting from entanglement. Upon exposure to mechanical stresses, the EPM network undergoes disentanglement of the EPM chains and is subject to chain slippage and flow. As expected for elastomer-containing blends, both EPM- and SEBS-compatible PP/PA-6 blends gave improved notched Charpy impact strength which increases with increasing volume fractions of SEBS-g-MAH or EPM-g-MAH respectively. At identical volume fractions, the more stiffer SEBS was much more efficient as impact modifier. For example, with 15 vol.-% SEBS-g-MAH the notched Charpy impact strength increased by more than one order of magnitude and reached 90 kJ/m<sup>2</sup> in comparison to 55 kJ/m<sup>2</sup> impact strength for EPM-based PP/PA-6 blends.

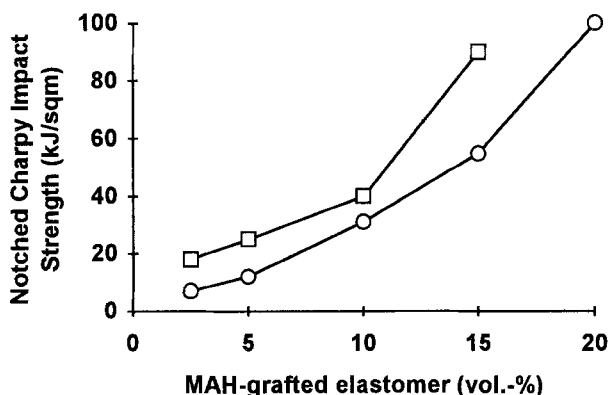


Figure 5. Influence of SEBS-g-MAH- (□) and EPM-g-MAH- (O) addition on the impact strength of PP/PA-6 (70/30) blends.

At 20 vol.-% SEBS-g-MAH content the PP/PA-6 blend sample does not fail in the impact pendulum test. The crack stopped after propagating half way through the sample. Near the crack tip the stress-whitened zone reflected extensive plastic deformation. This behavior was not paralleled by the corresponding EPM-based blends. The superior performance of SEBS-g-MAH impact modifiers may result from both better interfacial adhesion and substantially smaller core/shell microparticles which appear to be efficient stress concentrators.

Concerning the stiffness/toughness balance, the SEBS-g-MAH compatibilizers clearly outperform the EPM-g-MAH compatibilizers over the entire volume-fraction range. For a given Young's modulus of 1000 MPa, SEBS-based blends reached notched Charpy impact strength of 40 kJ/m<sup>2</sup> while the EPM-based blends gave only 12 kJ/m<sup>2</sup> impact strength which was only a marginal improvement in comparison to the PP matrix with 6 kJ/m<sup>2</sup>. Moreover, blends with 50 kJ/m<sup>2</sup> impact strength exhibited Young's modulus of 950 MPa for SEBS-based blends, whereas EPM-based blends with the same impact strength were extremely soft with Young's modulus of 590 MPa. As a rule, the relationship between Young's modulus and impact strength was drastically different for SEBS- and EPM-compatible PP/PA-6 (70/30) blends. This stiffness/toughness balance is closely related to both volume fraction and stiffness of the elastomer shells. Since the Young's modulus of SEBS is twentyfive-fold higher than that of EPM, also the PA-6/SEBS-core/shell microparticles are much stiffer than the corresponding PA-6/EPM microparticles. Therefore the stiffness of SEBS-compatible PP/PA-6 (70/30) blends is retained while the soft

EPM compatibilizer drastically reduces blend stiffness. For example, 5 vol.-% SEBS-g-MAH reduce the Young's modulus of the PP matrix from 1150 to 1000 MPa, while both impact strength and yield stress increase substantially.

In addition to stiffness of the elastomeric compatibilizer, also the efficiency as dispersing agent plays an important role. With SEBS-g-MAH much smaller core/shell microparticles are obtained. Consistent with earlier research on elastomer-modified PP, reported by Karger-Kocsis and Csikai (11) for PP/EPM-blends, the impact strength improves with decreasing average diameters of the dispersed elastomer microphases. In conclusion, the SEBS-g-MAH is an efficient dispersing agent for PA-6 in PP-melts, thus producing SEBS-compatible PA-6 microparticles of very small average diameter and narrow particle size distribution. Such in-situ formed PA-6/SEBS core/shell microparticles possess excellent interfacial adhesion and provide efficient transfer of mechanical stresses between PA-6 and the PP matrix. Therefore, the ternary PP/PA-6/SEBS-g-MAH blends exhibit unusual blend synergisms of high toughness and strength without sacrificing stiffness.

## References

- 1) Echte A, *Angew. Makromol. Chem.* (1977), 58/59, 175
- 2) Schmidt B, *Angew. Chem. Int. Ed. Engl.* (1979), 18, 273
- 3) Retting W, *Angew. Makromol. Chem.* (1977), 58/59, 133
- 4) Menzel G, in "Plastics Additives", Gächter R, Müller H (eds.) Hanser Publ. Co., Munich 2nd ed. (1984) chapter 8, p. 361
- 5) Hobbs SY, Dekkers MEJ, Watkins VH *Polymer* (1988), 29, 1598
- 6) Nakagawa H, Sano H, *Am. Chem. Soc., Polym. Chem. Div. Polym. Prepr.* (1987), 26(2), 249 - 250.
- 7) Bucknall CB, Cote FFP, Partridge JFK *J Mater. Sci.* (1986) 21, 301
- 8) Matonis VA, Small NC *Polym. Eng. Sci.* (1969) 9, 90
- 9) Scott CE, Macosko CW *Polym. Bull.* (1991) 26, 341
- 10) Nielsen LE J. *Appl. Polym. Sci.* (1966) 10, 97
- 11) Karger-Kocsis J, Csikai I *Polym. Eng. Sci.* (1987) 27, 241

**Accepted March 3, 1994 C**